

Debris Disks in Kepler Exoplanet Systems

S. M. Lawler¹, B. Gladman¹

ABSTRACT

The Kepler Mission recently identified 997 systems hosting candidate extra-solar planets, many of which are super-Earths. Realizing these planetary systems are candidates to host extrasolar asteroid belts, we use mid-infrared data from the Wide-field Infrared Survey Explorer (WISE) to search for emission from dust in these systems. We find excesses around eight stars, indicating the presence of warm to hot dust (~ 100 -500 K), corresponding to orbital distances of 0.1-10 AU for these solar-type stars. The strongest detection, KOI 1099, demands ~ 500 K dust interior to the orbit of its exoplanet candidate. One star, KOI 904, may host very hot dust (~ 1200 K, corresponding to 0.02 AU). Although the fraction of these exoplanet-bearing stars with detectable warm excesses ($\sim 3\%$) is similar to that found by Spitzer surveys of solar-type field stars, the excesses detectable in the WISE data have much higher fractional luminosities (L_{dust}/L_*) than most known debris disks, implying that the fraction with debris disks of comparable luminosity may actually be significantly higher. It is difficult to explain the presence of dust so close to the host stars, generally corresponding to dust rings at radii < 0.3 AU; both the collisional and Poynting-Robertson drag timescales to remove dust from the system are hundreds of years or less at these distances. Assuming a steady-state for these systems implies large mass consumption rates with these short removal timescales, meaning that the dust production mechanism in these systems must almost certainly be episodic in nature.

1. Introduction

The evolution of solid circumstellar material is a competition between the accretional processes that form planets (when speeds are low) and the violent collisional processes which in post-formation systems inexorably grind down the material into particles small enough that radiation forces can remove them from the system. The disappearance of infrared

¹University of British Columbia, Department of Physics and Astronomy, 6244 Agricultural Road, Vancouver, BC V6T 1Z1 Canada

(IR) excesses around forming stars (on 3-10 Myr time scales) occurs because the accretional processes win and sequester the huge mass of dust into a (relatively) tiny number of objects with very low surface area/mass ratios. In contrast, the observed debris disks (known around hundreds of solar-type stars) are thought to be from collisional dust production as velocities rise during the final stages of planet assembly (for relatively young stars), or triggered around older stars as dust is liberated in higher-speed collisions (Wyatt 2008). It is these more mature systems where our understanding of the physical picture is arguably incomplete. Although only $\sim 2\%$ of nearby main-sequence stars have massive detectable warm disks ($>200\text{K}$; Lawler et al. 2009), several of these disks require dramatic hypotheses to produce the large dust mass estimated. That is, estimates of the collisional grinding of small-body belts indicate that the systems in question should not still possess dust at anywhere near the observed level (Wyatt et al. 2007). In fact, Rhee et al. (2008) went so far as to liken the dust mass around BD +20 307 as a ‘miracle’ given collisional-model predictions.

Debris disks are detected and studied via the excess IR flux they produce in the system, caused by the dust re-radiating the absorbed stellar light. This dust emission can then dominate the stellar photosphere in the IR, where the dust’s blackbody peak is set by the equilibrium temperature at the orbital distance (for a narrow ring) or at an extended disk’s inner edge, because the warmest dust usually dominates the systems dust emission. For ‘realistic’ (although uncertain) dust grain size distributions, cross-sectional area and thus thermal emission is dominated by small grains, but the system mass is dominated by the unconstrained larger bodies. The true observable is thus the mass in grains in the decade larger than the peak wavelength.

Known disk systems consist of two types. The most common are massive and cold, analogous to the Solar System’s Kuiper belt. A few hotter ($T > 200\text{K}$) systems are known, which are massive cousins of our asteroid belt. An example is HD 69830, hosting 3 RV-discovered Neptune-mass planets inside 0.6 AU (Lovis et al. 2006) and a warm dust ring at ~ 1 AU, with an estimated $4 \times 10^{-7} M_{\oplus}$ in small grains alone (Lisse et al. 2007). Production of this dust is problematic (Beichman et al. 2005), with hypotheses ranging from comet swarms to super-comets to massive planetary collisions; it is difficult to judge the plausibility of these mechanisms given the rarity of these outcomes.

Dust grains in orbit around a star are quickly destroyed, and must be replenished by a fragmentation cascade, where asteroids within a belt collide and break into progressively smaller pieces (Wyatt 2008). The lifetime of a debris disk will be the same as the lifetime of the largest bodies in the source population that are available to be pulverized into dust grains. Very small grains ($\lesssim 1 \mu\text{m}$) are quickly blown away by stellar radiation pressure. Larger grains suffer Poynting-Robertson (PR) drag and spiral into the star in much less

than the system’s age; for dust very close to the star (~ 0.1 AU), orbits collapse in only hundreds of years.

In this paper we search for excess infrared emission, indicating the presence of a dusty debris disk, in systems found by the Kepler mission to possess transiting exoplanets. In Section 2 we define our sample and discuss our methodology for identifying excess candidates, and in Section 3 we provide additional details on the eight stars that have excesses. Section 4 contains a discussion of the problems associated with having this much dust so close to the host star, and finally Section 5 contains a summary of recent work and this study’s contribution relating debris disks to the presence of exoplanets.

2. WISE Data

WISE released preliminary survey data in April 2011, covering about half the sky in photometric bands centered on 3.4, 4.6, 12, and 22 μm (W1, W2, W3, and W4, respectively; Wright et al. 2010). Due to the pointing strategy of the telescope, the coverage on the sky is non-uniform. Many individual images are stacked to produce the preliminary survey data, and some areas of the sky were visited more often than others, providing deeper coverage in those areas.

2.1. Defining Our Sample

We use WISE data to search for dust emission around the 928 solar-type stars (F, G, and K0-7 spectral types; $T_{\text{eff}}=4000\text{-}7200$ K) that have stellar data (T_{eff} , metallicity, and $\log(g)$) reported in the Kepler database as of November 2011 and are candidates to host one or more planets contained in the first Kepler data release (Borucki et al. 2011; Lissauer et al. 2011b). Although most of these transiting planet candidates remain to be independently confirmed, we will refer to them as planets for brevity. The false-positive rate for single planet systems is $<10\%$ (Morton and Johnson 2011), and is much lower for multiplanet systems (Ragozzine and Holman 2010; Lissauer et al. 2011a). In any case, the existence or lack of planets is irrelevant for our analysis of IR excess.

There are several M stars reported as having planets in the Kepler database, but we did not consider these for analysis because of known systematic problems with modeling the atmospheres of such cool stars (Beichman et al. 2006a; Sinclair et al. 2010). We also did not consider the few hotter (A-type) stars with known Kepler planets in order to keep to stars similar to our Sun.

The WISE preliminary data release covers about half the Kepler field, detecting 439 out of the 928 solar-type stars; we consider a target to be ‘detected’ in a given band if the WISE Source Catalog reports a signal-to-noise ratio (SNR) greater than 3. (WISE does not report fluxes, but rather magnitudes and their corresponding magnitude uncertainty.) All WISE detections are within 1 arcsecond of the coordinates given by the Kepler team. The band wavelengths cover where hot dust emission would peak, which in these systems is also near the equilibrium temperatures of the known Kepler planets, most of which are located 0.01-0.4 AU from their host stars (Lissauer et al. 2011b).

134 of these stars were flagged by the WISE team as having contamination from nearby, bright stars in the form of a halo or diffraction spike, or flagged as extended, suggesting probable contamination by a background object. These stars were not considered further.

The remaining 325 stars are all detected in both WISE’s W1 ($3.4\ \mu\text{m}$) and W2 ($4.6\ \mu\text{m}$) bands, $\sim 2/3$ of these are also detected in W3 ($12\ \mu\text{m}$), and only six are also detected in W4 ($22\ \mu\text{m}$).

2.2. Finding Excesses in the WISE Data

To determine if the WISE data match the expected stellar photospheric spectrum or represent an excess of emission, we use Kurucz stellar atmosphere models (Castelli and Kurucz 2004) chosen from a grid of stellar temperatures, surface gravities, and metallicities to closely match those given for each star in the Kepler online database (Brown et al. 2011). The Kurucz models are scaled using photometry from the Sloan Digital Sky Survey (SDSS; Abazajian et al. 2009) and the Two Micron All-Sky Survey (2MASS; Skrutskie et al. 2006). These Kepler targets are more distant than most known debris disk hosts (hundreds of parsecs), so extinction must be taken into account. The Kepler database provides $E(B - V)$ measurements for each star, which we scale for each photometric band (Rieke and Lebofsky 1985) and use to correct the photometry. The Kurucz model is scaled to each star’s flux using the corrected photometry, and then convolved with the efficiency function over each WISE passband. The band zero points then provide expected magnitudes.

There are several sources of error in these measurements. To estimate magnitude uncertainties δ , the given error bars for each datapoint (δ_W) and the WISE absolute photometric errors (2.4, 2.8, 4.5, and 5.7% in W1-4, respectively; Wright et al. 2010) are added in quadrature. To assess the significance of each possible excess, the WISE magnitude (m) is subtracted from the predicted stellar magnitudes (m_{pred}), and this is divided by the uncertainty (δ) in that band to give a dimensionless excess. Our sign choice results in positive

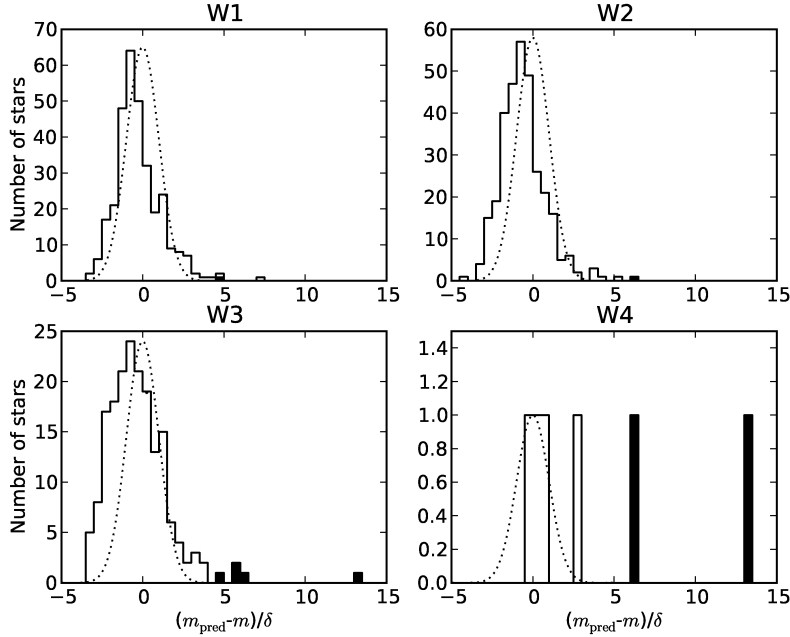


Fig. 1.— The excess significances for each band $(m_{\text{pred}} - m)/\delta$. Overplotted are Gaussians with width δ for reference. Small ($\sim 1 \delta$) systematics are still clearly present. Filled bars show what we accept as significant excesses. One system (KOI 379) shows excess in W1 and W2 above the 5δ level (7δ in W1 and 5δ in W2) but is not considered to be significant because of an obvious large flux mismatch between the SDSS and 2MASS photometry, perhaps indicating stellar variability.

excesses indicating that the WISE flux is higher than the predicted flux. The uncertainties in the stellar measurements reported by the Kepler database are ± 200 K in temperature and 0.4 dex in $\log(g)$ (Brown et al. 2011). We estimated the contribution of these uncertainties to the significance of the WISE excesses by using stellar models from $(T_{\text{eff}}, \log(g))$ gridpoints that were varied by the error bars in each of these parameters, and we found that this resulted in $< 1 \delta$ changes in the excess. In order to account for this without having a formal number to add to our errors, we adopt the fairly stringent requirement that in order for an excess to be considered significant, it must be more than 5δ above the photospheric magnitude.

Because of the large photometric aperture on the WISE measurements (8.25 arcseconds for W1-W3 and 16.5 arcseconds for W4), we visually inspected both the WISE and SDSS images for each of the stars we find to have an excess and found that there is not contamination from any nearby, bright stars. In addition, we checked to make sure there were not

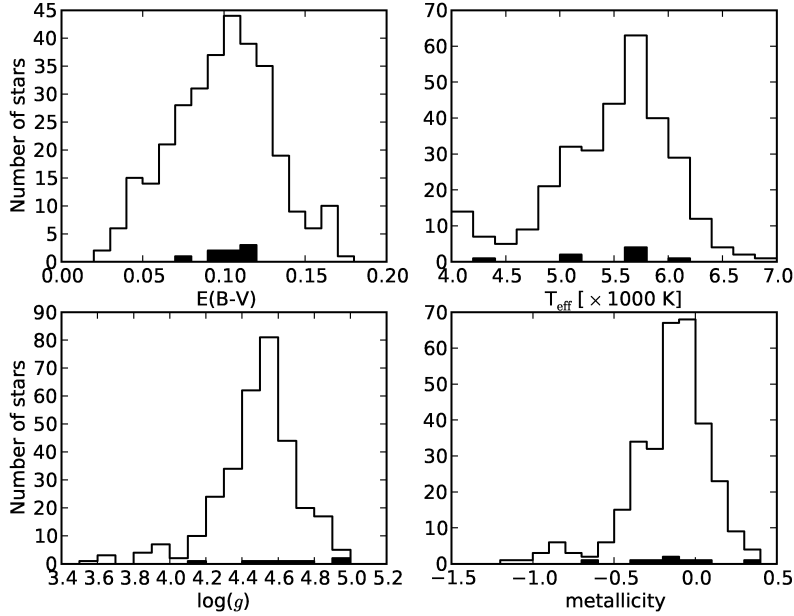


Fig. 2.— Histograms of each of the four stellar parameters reported by the Kepler team. Filled bars show these values for the eight systems with significant excess in at least one WISE band. There appear to be no correlations between the presence of a significant excess and any of these parameters.

systematic offsets in the expected position of the stars with excess, indicating contamination by a nearby background source.

The distribution of excesses for each band are shown in Figure 1. They follow approximately Gaussian distributions, with very few datapoints falling above 5δ and none falling below -5δ . Figure 1 makes it clear that the systematic error here actually underestimates the significance of the excesses; if anything we are being more conservative with our definition of what is a significant excess and what is not.

Figure 2 shows stellar properties for our sample as reported by the Kepler team: extinction, stellar temperature, surface gravity, and metallicity. No trends are seen between any of these data and the presence of a significant excess in any band.

3. Candidate Debris Disk Detections

The vast majority of stars we examined have WISE fluxes consistent with the photo-

Table 2. Debris Disk Candidates

KOI	Kepler Data					10 μm BB Dust Ring Model ^a				1 μm Mod. BB Dust Ring Model ^b			
	Stellar		Planetary			Dust Properties				Dust Properties			
	sp. type ^c	extinction $E(B - V)$	a [AU]	radius [R_{\oplus}]	mass ^d [M_{\oplus}]	T [K]	a [AU]	M [M_{\oplus}]	L_d/L_* [$\times 10^{-3}$]	T [K]	a [AU]	M [M_{\oplus}]	L_d/L_* [$\times 10^{-3}$]
904 ^e	K5	0.074	0.029 0.159	2.1 3.0	5 10	1200 ^f	0.02	1×10^{-8}	13	1100 ^f	0.02	2×10^{-9}	15
469	G0	0.116	0.095	5.5	35	400 ^f	0.36	8×10^{-7}	3	300 ^f	0.64	2×10^{-7}	3
559	K0	0.099	0.052	1.4	2	471	0.23	4×10^{-7}	4	382	0.34	1×10^{-7}	4
871	G5	0.092	0.105	10.9	144	329	0.27	6×10^{-7}	4	283	0.37	1×10^{-7}	4
943	K0	0.102	0.045	2.2	5	357	0.28	1×10^{-6}	6	303	0.39	2×10^{-7}	6
1099	G5	0.114	0.573	3.7	15	487	0.14	6×10^{-7}	14	394	0.22	1×10^{-7}	14
1020	G3	0.11	0.294	21.9	614	100 ^f	9.89	5×10^{-4}	3	90 ^f	12.21	6×10^{-5}	2
1564	G4	0.109	0.275	3.1	11	135 ^f	1.96	1×10^{-4}	16	115 ^f	2.70	2×10^{-5}	14

^aAssuming blackbody dust grains of radius 10 μm ^bAssuming modified blackbody dust grains of radius 1 μm ^cSpectral type is approximate and based on the stellar temperature provided by the Kepler team^dPlanet mass is calculated according to $M/M_{\oplus} = (R/R_{\oplus})^{2.08}$ (Borucki et al. 2011)^eKOI 904 has two known planets, both of which are listed here^f T_{dust} is assumed rather than fit. See text for details on each system.

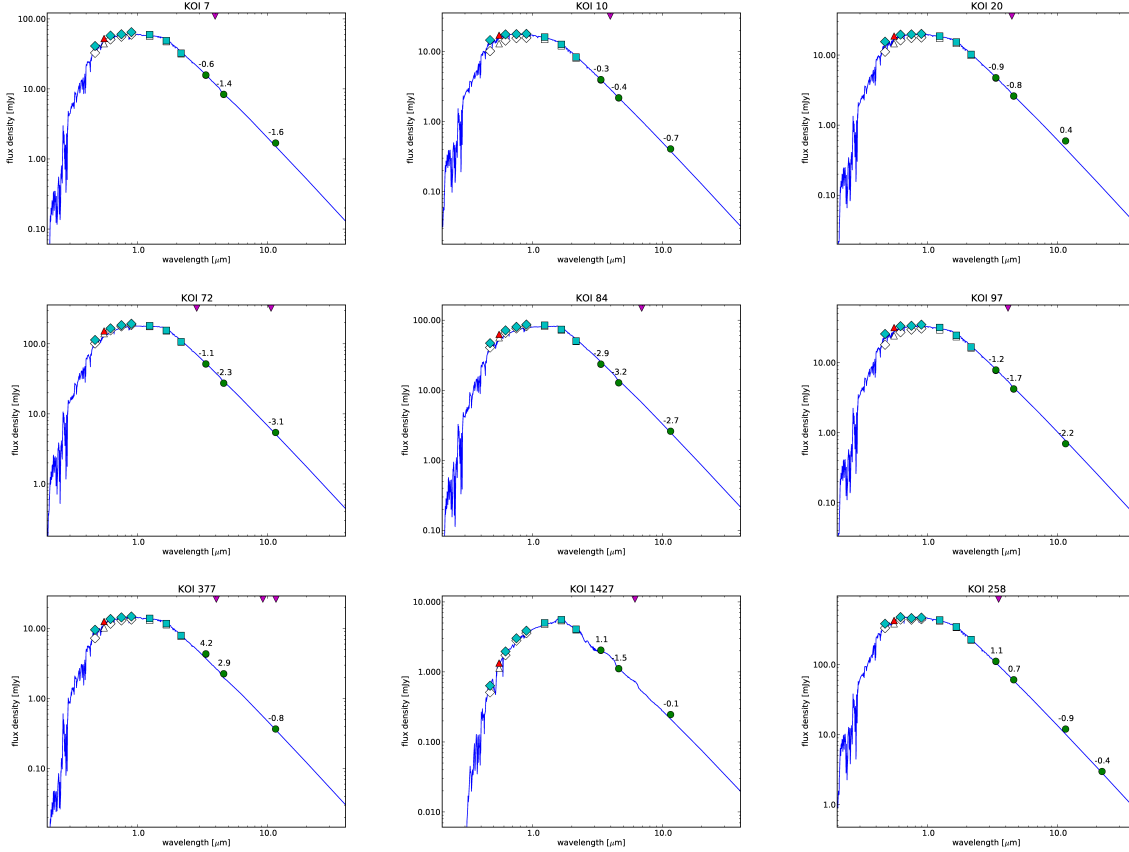


Fig. 3.— Nine stars with WISE data that is consistent with the stellar photosphere. Included here are all of the confirmed systems that currently (as of November 2011) have WISE data (none of these systems have significant excesses): KOI 7 = Kepler 4 (Borucki et al. 2010), KOI 10 = Kepler 8 (Borucki et al. 2010), KOI 20 = Kepler 12 (Fortney et al. 2011), KOI 72 = Kepler 10 (Batalha et al. 2011), KOI 84 = Kepler 19 (Ballard et al. 2011), KOI 97 = Kepler 7 (Borucki et al. 2010), and KOI 377 = Kepler 9 (Holman et al. 2010). KOI 1427 and KOI 258 are included as additional examples, being one of the coolest and warmest stars in the sample, respectively. Blue curve represents the stellar spectrum model. Cyan diamonds and squares show the SDSS and 2MASS data respectively used to scale the stellar model, and the red triangle shows the Kepler visual magnitude estimate converted to flux. The filled symbols show the extinction-corrected data, and the empty symbols show the original measured values. Green filled circles show the WISE data, and the error bars are often smaller than the datapoints. The excess (in multiples of δ) of the observed-predicted magnitudes are given for the stellar model above each WISE datapoint. At the top, triangles show the planetary thermal emission wavelength peak for reference.

sphere (these are listed in Table 1 and a selection of these stars are shown in Figure 3). In our full sample, we find eight stars with an excess of 5 δ or higher in at least one band. Unsurprisingly, these excesses generally appear in the longest two wavelength bands. These stars are listed in Table 2, the WISE data for each of these systems are listed in Table 3, and we discuss each of them in Sections 3.1-3.3 below.

Many simple debris disk models have been made using blackbody dust grains (i.e. Beichman et al. 2006b; Hillenbrand et al. 2008; Lawler et al. 2009). We adopt 10 μm radius blackbody dust grains for an initial model, both for ease of comparison with previous literature and for simplicity given the lack of spectral data. These models are not attempting to find the highly unconstrained ‘best’ possible dust model due to the myriad of complications inherent in dust emission (composition, radial distribution, emission features, and grain size), but rather to prove that the presence of dust provides a physically plausible model that approximately reproduces the WISE measurements. A single temperature blackbody is scaled to fit the WISE photometry, giving L_{dust}/L_* , which is used to calculate the area of absorbing dust σ_{dust} using $\sigma_{\text{dust}} = 4\pi a^2 L_{\text{dust}}/L_*$ (Wyatt 2008). When a density and radius are assumed for the grains, this can be converted to the mass in dust. We used 3.3 g cm^{-3} for silicate dust grains. The temperature changes the wavelength of the peak of the curve. The orbital distance of the dust is then calculated using the same assumptions as were used to calculate Kepler planet temperatures (albedo of 0.3, uniform surface temperature, and no atmospheric effects; Borucki et al. 2011).

It is probable that smaller grains are present, and if they dominate in the size distribution of dust grains, the dust could be significantly farther out and produce the same fit. We show this uncertainty in Table 2, where in addition to the best-fitting 10 μm dust grain model we show the best fit for a disk made of 1 μm modified blackbody dust grains, where the emissivity of the grains drops proportional to $(\lambda/\lambda_0)^{-\beta}$, with λ_0 equal to the grain size and β equal to 1 (Dent et al. 2000). This means that the spectral energy distribution resulting from these grains is the same as a blackbody for wavelengths shorter than 1 μm , and drops off more steeply than a blackbody at larger wavelengths. Smaller grains may be more realistic, as resolved disk studies have found larger disks than predicted by fitting a blackbody spectrum to the mid-IR excess (i.e. Krist et al. 2010). However, in the interest of picking a uniform model that can be compared with previous Spitzer studies, we use the 10 μm blackbody dust model for most of our calculations.

For our 10 μm dust grain model, the resulting blackbody curve is added to the stellar atmosphere model, and this is used to fit the WISE data. For most systems, the temperature and surface area of the emitting dust are both free parameters in the fit. Because in some systems there is only one datapoint that rises off the photosphere, the temperature cannot

be determined uniquely even if an upper limit can be set. These systems are noted in Table 2 and discussed below. For all eight systems, the fit for temperature is fairly unconstrained; the longest wavelength datapoint is almost always still rising, allowing a large number of cooler blackbody curves from more massive dust disks to pass through the datapoints. Thus the temperatures we calculate should be thought of as upper limits, as a larger amount of somewhat cooler dust could also produce the observed emission.

Using this simple dust model, the dust masses needed to produce these excesses range from $\sim 10^{-8}$ – 10^{-4} Earth masses, orders of magnitudes larger than the dust mass of our solar system ($\sim 4 \times 10^{-10} M_{\oplus}$; Hahn et al. 2002), and comparable in mass to known debris disk systems (typically 10^{-8} – $10^{-2} M_{\oplus}$; Beichman et al. 2005; Bryden et al. 2006; Wyatt et al. 2007; Rhee et al. 2008; Hillenbrand et al. 2008), but with higher fractional luminosities as shown in Figure 4.

We find that our eight excess systems can fit into three categories based on dust temperature (and thus dust location). For much of the literature, >200 K dust is considered to be hot dust. Due to the large variation in debris disk temperatures and terminology, for this paper we define our debris disk categories as the following: hot (~ 1000 K), warm (~ 300 – 500 K), and cool (~ 100 K). We now discuss each excess system in turn.

3.1. Warm Dust Systems (~ 300 – 500 K)

Because of its wavelength range, WISE is most effective at detecting dust temperatures between 300–500 K, similar to the handful of warm debris disks discussed in Wyatt et al. (2007). Figures 5 and 6 show the five systems that possess excesses consistent with emission by warm dust. Not surprisingly, due to the low photospheric flux predicted at long wavelengths, none of these systems have W4 detections with $\text{SNR} > 3$. The low SNR datapoints and upper limits that are plotted (but not included in our fit) give tantalizing hints of what the upcoming full WISE data release could reveal about the dust locations in these systems. The W4 datapoints may reveal that these systems are actually similar to the cool dust systems in dust mass and temperature (see Section 3.2). Only one of these five systems (KOI 1099) *requires* dust warmer than >300 K (see discussion below); in the other four systems we may be seeing the Wein tail of a cooler, more massive dust ring.

With the currently available WISE data, we find that these disks are plausibly hotter than the majority of known debris disk systems, and our best fitting models place dust on orbits of a few tenths of an AU. This is perhaps not surprising, as it is similar to the orbital radii of the known planets in these systems, so the dust may be co-located with several Earth

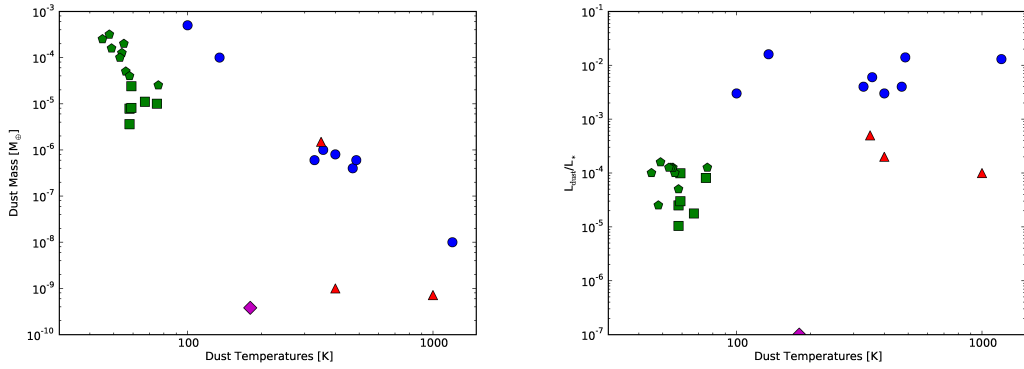


Fig. 4.— The derived masses, fractional luminosities, and temperatures of dust rings in our sample (using $10\ \mu\text{m}$ radius grains) compared to other known systems. Red triangles show systems examined by Wyatt et al. (2007) (see also Beichman et al. 2005, 2006b; Lisse et al. 2012), green squares are from a Spitzer spectroscopic survey (Lawler et al. 2009), and green pentagons are from a Spitzer photometric survey at $70\ \mu\text{m}$ (Hillenbrand et al. 2008). For comparison, the purple diamond shows zodiacal dust in our solar system (Hahn et al. 2002). All systems shown are mature, solar-type stars. Blue circles show the dust models presented in this paper. Because M_{grain} is proportional to grain size r_{grain} , using smaller grains would result in lower total dust masses (see Table 2). While the masses shown here are similar to known systems, because of the warmer temperatures we find for these Kepler systems, the resulting fractional luminosities L_{dust}/L_* are much higher.

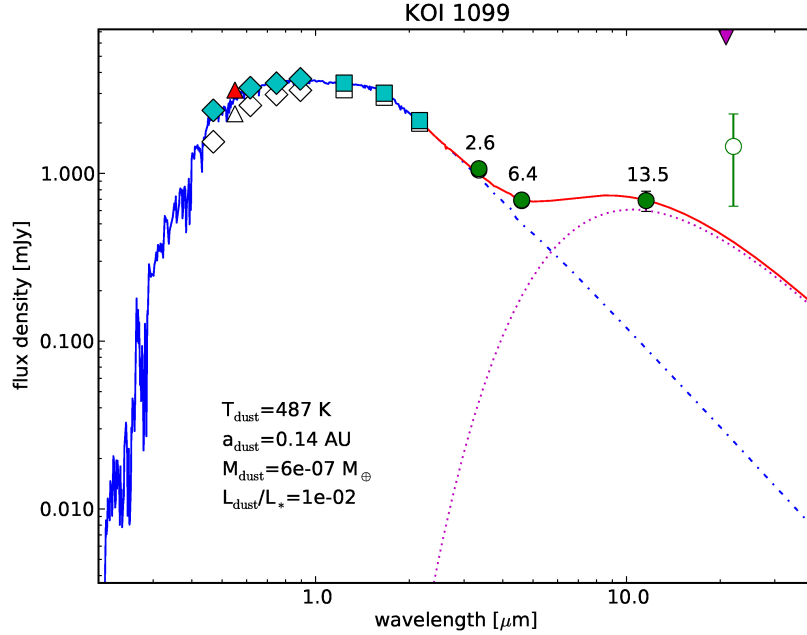


Fig. 5.— KOI 1099, our best candidate for a debris disk due to the strong excess in W2 and W3, and a weak excess in W1. See caption for Figure 3. The excess values (in multiples of the total magnitude uncertainty δ) for the stellar atmosphere model predictions (not including the dust model) are shown above each WISE datapoint. Additionally, the purple dotted curve shows the blackbody spectrum of a thin ring of $10 \mu\text{m}$ -radius dust grains, and the solid red curve shows the star+dust spectrum. The best-fitting dust mass, temperature, and orbital distance are also shown. The unfilled WISE datapoint shows $\text{SNR} < 3$ data that was not used in the fit, but gives a preview of where the upcoming WISE full data release may provide significant data.

masses of planetary material. Most systems in the literature known to host both a debris disk and one or more exoplanets have a large separation (tens of AU) between the orbit of the planet(s) and the debris disk (Bryden et al. 2009; Dodson-Robinson et al. 2011). One of the five systems in our sample with warm excesses has the modeled dust ring interior to the known planet (Figure 5), with four exterior (Figure 6). All planets are within a few tenths of an AU of the modeled debris disk, which may allow dynamical interactions between the planet and the disk.

The G5 star KOI 1099, shown in Figure 5, is our most promising candidate to host a debris disk, appearing to have excesses in all WISE bands. The weak excess in W1 combined with highly significant excesses in both the W2 and W3 bands demands dust emission of

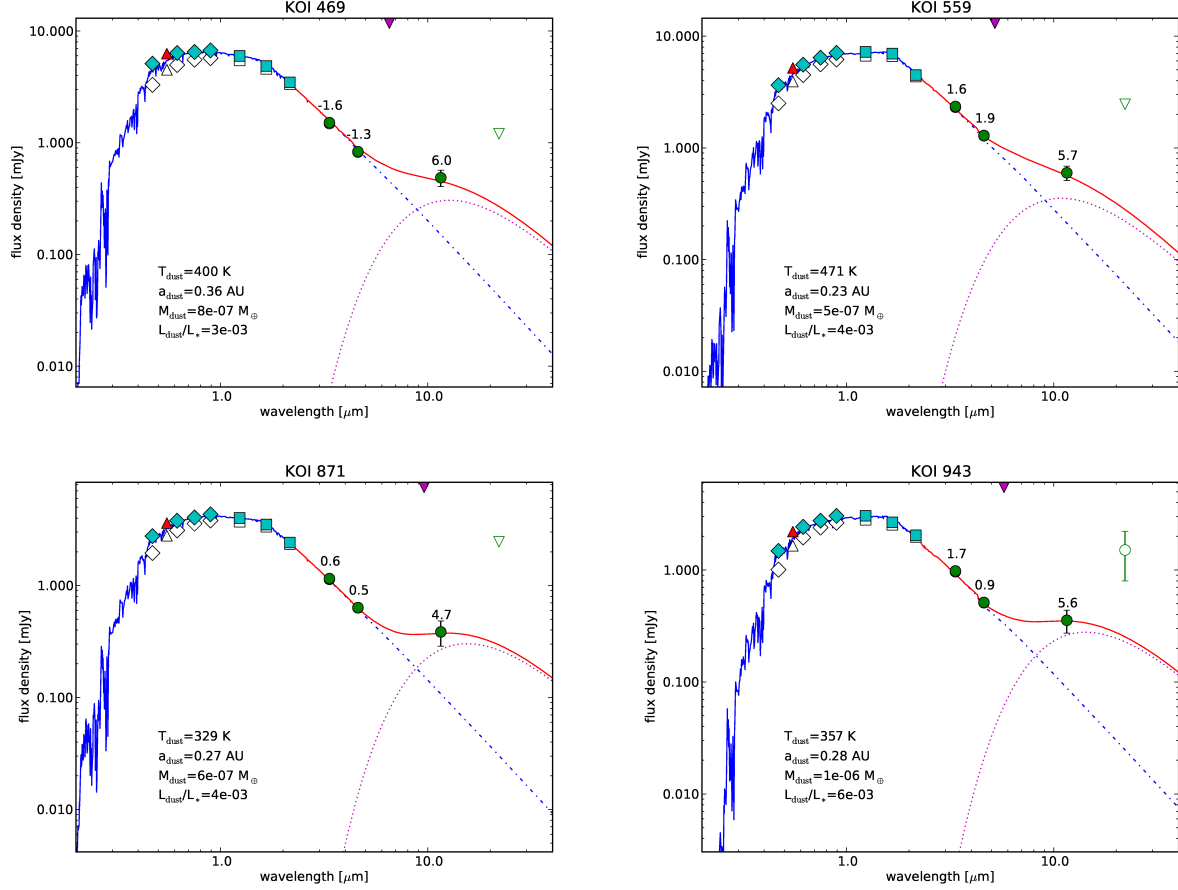


Fig. 6.— Stars with warm excesses, at orbital distances similar to that of the known planets. See captions for Figures 3 and 5. Open green triangles show upper limits on the W4 data, while open circles show W4 data with $\text{SNR} < 3$.

~ 500 K using our nominal model. An excellent match to all photometry between 0.5–12 μm is provided by a confined dust ring at 0.14 AU, although more complex distributions are certainly possible. The 1 μm modified-blackbody alternate model results in a cooler temperature (~ 400 K) and larger orbital radius for the dust ring (0.22 AU). Either model results in a ring is inside the 0.57 AU orbit of the known Neptune-mass planet (candidate), and may point to inspiral of dust past the planet from a more distant dust source. The W4 flux has $\text{SNR} < 3$ and so was not used in our fit, but if future WISE data releases confirm the ~ 1.5 mJy flux, this points to an even greater dust mass, much of which would be at larger distances from the star. Using the low SNR W4 datapoint along with the other WISE bands would not allow a single temperature fit, simply indicating that this system contains dust that is producing significant emission at more than one orbital distance.

The other four warm systems, shown in Figure 6, do not have formally significant W1 and W2 excesses. It is possible that these weak W1 and W2 excesses should be ignored, in which case the W3 excess is the start of a blackbody of a much more massive but colder disk. We evaluate this explicitly for the KOI 943 system, where there is a low-SNR W4 datapoint rather than just an upper limit.

KOI 469 is a G0 type star with a super-Neptune at 0.095 AU. Because only the W3 datapoint is off the photosphere (with only an upper limit in W4), for our best-fitting dust ring we fixed the temperature by eye and fit the data by scaling the mass of the ring. This gives a dust ring at 0.36 AU, outside the orbit of the known planet.

KOI 559 is a K0 type star with a $\sim 2 M_{\oplus}$ planet at 0.05 AU. There is a very weak excess in W1 and W2, with a strong excess at W3 and only a W4 upper limit. The best-fitting dust ring sits at 0.23 AU, well outside this hot super-Earth’s orbit.

The G5 star KOI 871 has a Saturn-mass planet at 0.1 AU. The WISE data is similar to KOI 559, with a very weak excess in W1 and W2, a strong excess in W3, and a W4 upper limit. The best fitting dust ring sits at 0.27 AU, again outside the planet’s orbit.

The K0 star KOI 943 follows the usual pattern of weak excesses in W1 and W2, with a strong excess in W3. The best-fitting dust ring sits at 0.28 AU, outside the orbit of KOI 943’s super-Earth at 0.05 AU. The low-SNR W4 datapoint hints at a more massive, more distant dust ring that will perhaps be confirmed by the upcoming full WISE data release. Using the nominal 1.5 mJy W4 flux in the fit pulls down the temperature to about 150 K, corresponding to a ring at 1.5 AU with a mass of $10^{-4} M_{\oplus}$, similar to the cool dust systems described in Section 3.2.

The dust masses required for all of these systems are fairly low: $\sim 10^{-7}$ - $10^{-6} M_{\oplus}$, approximately equivalent mass to grinding a 10 km asteroid into 10 μm dust grains.

3.2. Cool Dust Systems (~ 100 K)

These systems (Figure 7) more closely resemble classical debris disk systems that have been studied extensively at longer wavelengths by Spitzer, with dust located at several AU, well outside the orbits of the known planets (Bryden et al. 2009; Dodson-Robinson et al. 2011). We find two stars in our sample with excesses that are consistent with blackbody peaks at the W4 effective wavelength of 22 μm or longer, and strongly significant W4 detections.

KOI 1020 is a G3 star, and is the only star which has a strong W4 excess and yet no W1-W3 excess. This would require the dust to be quite cool ($\lesssim 100$ K). Due to the

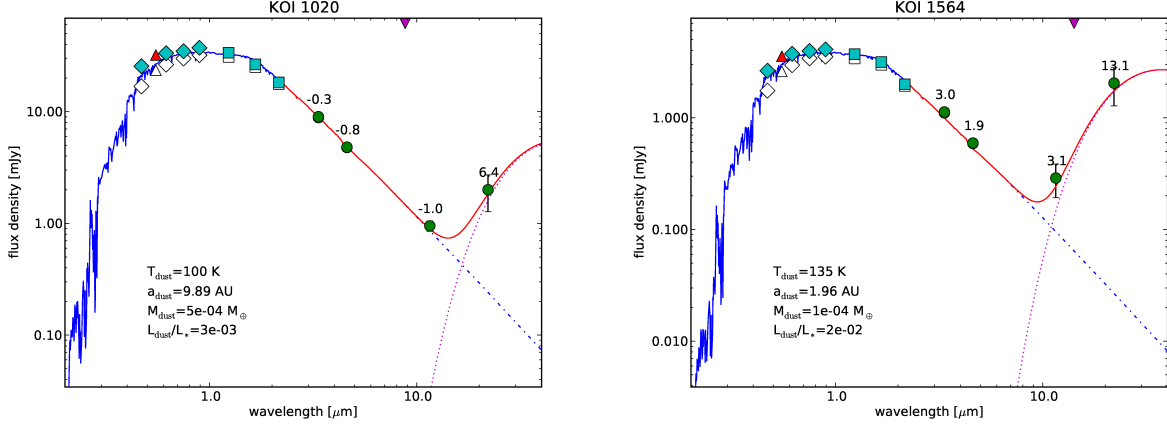


Fig. 7.— Stars with cool excesses (~ 100 K). See captions for Figures 3 and 5.

unconstrained temperature fit, we fixed T_{dust} at 100 K, but it could be colder if a more massive disk is present. Even the 100 K temperature places the dust at about 10 AU, far outside the orbit of its hot Jupiter at 0.3 AU.

KOI 1564 is a G4 star, and has weak excesses in each of the 3 shortest wavelength bands, with a large excess in W4. Due to the large error bars on the W3 and W4 data, there are quite a range of temperatures that fit, but our best dust model has an orbital distance of 2.0 AU. KOI 1564’s known Neptune-mass planet orbits well inside this, at 0.28 AU. The future improvement in the error bars provided by the next WISE data release will certainly better constrain this belt.

Both of these stars require high dust masses ($\sim 10^{-4} M_{\oplus}$) to produce the large excesses observed in W4, similar to the masses calculated for Spitzer surveys of solar-type stars at 24 and 70 μm (Bryden et al. 2006; Hillenbrand et al. 2008), although KOI 1564’s disk may be among the hottest known with this mass or larger.

3.3. Hot Dust (~ 1000 K) in a Multiplanet System

The K5 star KOI 904 (Figure 8) is the only multiplanet system to show an excess, as well as the only system with significant excess in the shortest wavelength band (3.4 μm). This alone requires extremely hot dust. Both of the planets are super-Earths, one at 0.03 AU and one at 0.16 AU, indicating that there is at least $\sim 15 M_{\oplus}$ of material near the star. Having two planets is significant, because it greatly reduces the possibility of a false positive exoplanet detection (Ragozzine and Holman 2010; Lissauer et al. 2011a). Currently, there is

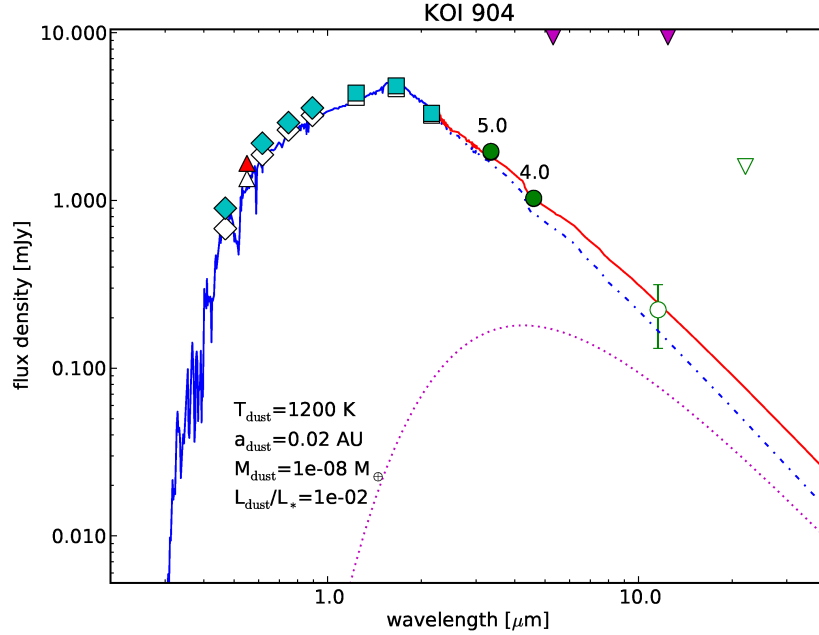


Fig. 8.— KOI 904: the only star with a strong excess in both W1 and W2, and the only multiplanet system in this sample to show an excess. See captions for Figure 3, 5 and 6.

not a detection in the W3 or W4 bands, only a low-SNR W3 point and a W4 upper limit, so the dust model is not well constrained. For lack of any other guidance on the temperature, we fixed it so the blackbody curve peaks near the W2 effective wavelength and found an acceptable fit. This results in very hot dust, close to the sublimation temperature of silicates. This exact temperature is uncertain, but must be quite hot (>1000 K) in order to fit both the W1 and W2 datapoints. But with currently only two datapoints, more detailed dust modelling is unwarranted.

This remains our most insecure excess; there is a small mismatch between the SDSS and 2MASS photometry which could be the result of stellar variability (although the star is not flagged as variable in the WISE database). This is among the cooler stars in the sample, and so there is the possibility of poor stellar atmosphere modeling, as for the M stars. However, other K5 and later stars appear in our sample without showing signs of excess in the WISE data (see Figure 2). The very hot dust is also a bit worrying, though it is not very different from the equilibrium temperature of the innermost known planet in this system (960 K), and dust temperatures in the range 500-1200 K have also been detected around white dwarfs (Chu et al. 2011).

If real, this very hot dust cannot be produced by planetesimals in orbit at this distance; as discussed in more detail in Section 4, both the collisional timescale and the Poynting-Robertson drag time guarantee that particles cannot stay in such close orbits to the star for more than hundreds of years.

Only a very small dust mass ($\sim 10^{-8} M_{\oplus}$) is required in this system because of the extremely hot temperatures. Dust this hot has only been observed with optical interferometers, and may actually be fairly common around solar-type stars (Defrère et al. 2011), but is difficult to observe. Excesses this hot may have been missed by Spitzer spectroscopic surveys, which assumed no excess was present at shorter wavelengths if no slope other than Rayleigh-Jeans was found in the short wavelength data (Beichman et al. 2006b; Lawler et al. 2009). This excess is perhaps similar to that found for HD 23514 (Rhee et al. 2008), which was also detected at short wavelengths only. The full WISE data release should provide a high SNR W3 datapoint; if it remains above the photosphere, the case for a tenuous, but very hot ring of small grains near the planets will be strengthened.

We note that as this paper went to press, the February 2012 Kepler data release (Batalha et al. 2012) provided 3 additional planets in this system, bringing the total number of planet candidates around KOI 904 to five, all within 0.2 AU.

4. Dust Production

For the systems with abundant dust interior to 1 AU, it is difficult to produce viable steady-state models with such a large mass of small grains remaining so close to their stars. The PR drag timescale for dust to spiral into the star is extremely short at these close distances:

$$t_{\text{PR}} = 200 \text{ yr} \left(\frac{r_{\text{grain}}}{10 \text{ } \mu\text{m}} \right) \left(\frac{a}{1 \text{ AU}} \right)^2 \quad (1)$$

for 3 g cm^{-3} grains (Burns et al. 1979), giving only ~ 10 years for $10 \text{ } \mu\text{m}$ grains at 0.25 AU (a typical orbital distance in Table 2). Inspiring grains would not ultimately reach the star in any case, as they should vaporize at $\sim 1000\text{--}1500 \text{ K}$ (depending on composition) once they get close enough for temperatures to rise this high. But even before reaching this sublimation temperature, the collisional lifetime may drop below the orbital timescale and dust will quickly be smashed into pieces smaller than the blowout limit.

This timescale (t_{coll}) for inter-grain collisions to produce fragments smaller than the blowout limit is very short at these orbital radii and number densities. For a completely coupled narrow ring of width $2ae$ and height $2ai$ where all grains have the same size r_{grain} , semimajor axis a , eccentricity e , and inclination i , t_{coll} can be approximated by the inverse

of the collision frequency, $n\sigma v$, where n is the number density of particles, σ is the cross-sectional area of one particle, and v is the relative speed between particles. This gives the scaling:

$$t_{\text{coll}} \sim 0.3 \text{ yr} \left(\frac{e}{0.1} \right) \left(\frac{\rho}{3 \text{ g cm}^{-3}} \right) \left(\frac{10^{-6} M_{\oplus}}{M_{\text{grain}}} \right) \left(\frac{r_{\text{grain}}}{10 \mu\text{m}} \right) \left(\frac{a}{0.25 \text{ AU}} \right)^{3.5} \quad (2)$$

where ρ is the density of a dust grain, M_{grain} is the total mass of the dust grains, and the approximation has been made that $e \approx i$ (where i is in radians). With $t_{\text{coll}} = 0.3 \text{ yr}$ for our typical warm systems, a steady state requires replenishing $\sim 10^{-6} M_{\oplus}$ (or more) of dust every year, consuming $>1000 M_{\oplus}$ of material in 1 Gyr, which is unreasonably large.

Unrealistic mass-consumption rates implied by such steady-state models are worrying, and have been noted for several main-sequence, warm debris disk systems. The fractional luminosities $L_{\text{dust}}/L_{\star}$ we measure for Kepler systems with excesses also greatly exceed the maximum predicted by the steady-state collisional model of Wyatt et al. (2007) given these stars’ mature ages. The common logical conclusion is that dust masses at this level have to be transient. Several theories have been proposed to explain such systems, including comet swarms, a “supercomet”, or a recent collision (HD 69830; Beichman et al. 2005), or a late-heavy bombardment-style dynamical instability forcing many icy bodies onto highly eccentric orbits, bringing them in close to the star where they collide or sublimate (η Corvi; Wyatt et al. 2007; Lisse et al. 2012).

Another possible explanation for these massive debris disks may be that these stars are all young ($<100 \text{ Myr}$) and still in the process of clearing their protoplanetary disks. This hypothesis was offered for three of the seven stars presented by Wyatt et al. (2007) with disks far too massive to be maintained by a steady-state collisional cascade. We inspected Palomar Sky Survey images and found no evidence that any of our sample stars are associated with the open clusters in the Kepler field, reducing the probability that this explains these systems.

A further option is that the dust may be impact ejecta from asteroids or comets recently striking the extant exoplanets, similar to the production of giant planet rings in our Solar System (Burns et al. 1999); however this is challenging given the super-Earths’ large escape speeds, even if impact speeds are also high.

What is clear is that these dust grains cannot be co-located with a planetesimal belt that is producing them. A massive asteroid belt at 0.2 AU or closer is an unsatisfactory dust source because t_{coll} for the planetesimals is $\ll 1 \text{ Gyr}$ (Wyatt et al. 2007; Moldovan et al. 2010) and the source would now be gone. Dust also cannot simply spiral in to these close distances from a more distant source in steady-state. The high optical depths that we

calculate must be present in these systems (ranging from $\tau \sim 0.01 - 0.5$) are several orders of magnitude higher than the maximum allowed (Wyatt 2005) in a steady-state inspiral scenario, meaning that the dust present in these quantities would destroy itself collisionally before PR drag has a chance to move it any significant distance.

Given the large dust masses and the small fraction of stars that possess these excesses, episodic dust production mechanisms provide the most attractive explanation. Dust could be produced by a catastrophic collision between asteroids located further from the star, and we are seeing the dust as it spirals in toward the star. However, the probability of occurrence required by this theory may not be high enough to explain the observed fraction of such systems. Dynamical instabilities forcing many bodies from the outer reaches of these solar systems onto eccentric orbits so they collide close to the star, perhaps similar in style to the Late-Heavy Bombardment in our Solar System, might be seen as an attractive theory. However, the fraction of systems observed to have $24 \mu\text{m}$ excesses observed by Spitzer appears to be much too high given the short lifetime of such an event (Booth et al. 2009).

5. Discussion

We find IR excesses around eight stars that also host planet candidates. The masses and luminosities of these excesses are all too large to be explained by a steady-state collisional cascade. Given that the WISE field coverage was not uniform in depth, and so many of these relatively faint stars suffered from contamination by nearby bright stars, it is challenging to say anything robust about the fraction of these planet-hosting stars that have excesses in our sample. Out of the 186 stars with W3 data of $\text{SNR} > 3$, five have significant $> 5 \delta$ excesses, or $\sim 3\%$. At first glance, this fraction appears similar to the 2% of solar-type stars with warm excesses (Wyatt et al. 2007; Lawler et al. 2009).

However, the fractional luminosities of these Kepler systems with excesses are much higher than most known debris disks (Figure 4 and Moór et al. 2006). Because of the larger distances and thus lower apparent brightness of these Kepler systems as compared to most known debris disk systems, only the brightest debris disks would be detected by WISE. Presumably the eight systems presented here are the very highest luminosity debris disks in the sample, and many more fainter disks are present around these planet-hosting stars. This would indicate that the fraction of stars possessing debris disks and Kepler-detected exoplanets is actually much higher than the fraction of field stars with debris disks.

Surveys with Spitzer (Bryden et al. 2009; Dodson-Robinson et al. 2011) have found that hosting a radial velocity-detected exoplanet does not make a star more likely to host a debris

disk, and a recent WISE survey of exoplanets discovered by ground-based transit searches (Krivov et al. 2011) has found that the fraction of these stars ($\sim 2\%$) to host warm debris disks (excesses in W3 and W4) is similar to that found by Wyatt et al. (2007).

The Kepler systems studied here are different from other disk-bearing exoplanet systems, whose planets are primarily discovered by the radial-velocity (RV) technique, and by ground-based transit searches. Exoplanets from the latter two techniques are mostly large and very close to their stars, with an average mass of ~ 2 Jupiter masses and $< 20\%$ known to be in multiplanet systems (Wright et al. 2011). The recently announced 1200 Kepler exoplanet candidates (Borucki et al. 2011) are in a different regime, with about $1/3$ in multiplanet systems, and having many super-Earths (typically 2-6 Earth radii) well inside 1 AU. Among our excess systems, all but two of the planets are Neptune mass or smaller; only one is massive enough to be a hot Jupiter. The resulting correlation we find between a star hosting both small planets and a debris disk inside a few AU agrees with the planetary formation and dynamical evolution models presented by Raymond et al. (2012). This makes sense in a picture where migrating Jupiters clean out the terrestrial systems they pass through.

Explaining the large dust masses required to produce these excesses remains a huge challenge. Steady-state theories appear to fail completely, as the mass consumption rates required would involve destroying thousands of Earth masses of planetary material over the lifetime of these stars. Episodic events such as catastrophic collisions between bodies may provide an explanation, but these events must last long enough and occur frequently enough to result in $\sim 3\%$ of solar-type stars in this state at any given moment. Much theoretical work needs to be done here.

The upcoming WISE full-sky data release will access additional systems, decrease the error bars on existing measurements, and provide longer-wavelength measurements for some of these systems to see if there is dust at larger orbital distances. Spectral data on these candidates would be invaluable, but the host stars are faint. Future Kepler data releases will contain planets on more distant orbits, perhaps yielding planets in closer proximity to these new debris disks.

The authors wish to thank Angelle Tanner, Ryan Goldsbury, Harvey Richer, Joe Burns, Casey Lisse, Alexander Krivov, Kate Su, and Geoff Bryden for helpful discussions, and an anonymous referee whose comments greatly improved our interpretation of the data. The authors wish to thank both the Kepler and WISE science teams not only for carrying out incredibly successful missions, but for making their data publicly available.

This paper includes data collected by the Kepler mission. Funding for the Kepler mission is provided by the NASA Science Mission directorate. Some of the data presented in this

paper were obtained from the Multimission Archive at the Space Telescope Science Institute (MAST). STScI is operated by the Association of Universities for Research in Astronomy, Inc., under NASA contract NAS5-26555. Support for MAST for non-HST data is provided by the NASA Office of Space Science via grant NNX09AF08G and by other grants and contracts. This publication makes use of data products from the Wide-field Infrared Survey Explorer, which is a joint project of the University of California, Los Angeles, and the Jet Propulsion Laboratory/California Institute of Technology, funded by the National Aeronautics and Space Administration. This publication also makes use of data products from the Two Micron All Sky Survey, which is a joint project of the University of Massachusetts and the Infrared Processing and Analysis Center/California Institute of Technology, funded by the National Aeronautics and Space Administration and the National Science Foundation. This research has made use of the NASA/ IPAC Infrared Science Archive, which is operated by the Jet Propulsion Laboratory, California Institute of Technology, under contract with the National Aeronautics and Space Administration.

This paper is dedicated to Sylvia Maria Bongarzone Lawler who was born December 23, 2011.

REFERENCES

- Abazajian, K. N., Adelman-McCarthy, J. K., Agüeros, M. A., Allam, S. S., Allende Prieto, C., An, D., Anderson, K. S. J., Anderson, S. F., Annis, J., Bahcall, N. A., and et al.: 2009, *ApJS* **182**, 543
- Ballard, S., Fabrycky, D., Fressin, F., Charbonneau, D., Desert, J.-M., Torres, G., Marcy, G., Burke, C. J., Isaacson, H., Henze, C., Steffen, J. H., Ciardi, D. R., Howell, S. B., Cochran, W. D., Endl, M., Bryson, S. T., Rowe, J. F., Holman, M. J., Lissauer, J. J., Jenkins, J. M., Still, M., Ford, E. B., Christiansen, J. L., Middour, C. K., Haas, M. R., Li, J., Hall, J. R., McCauliff, S., Batalha, N. M., Koch, D. G., and Borucki, W. J.: 2011, *ApJ* **743**, 200
- Batalha, N. M., Borucki, W. J., Bryson, S. T., Buchhave, L. A., Caldwell, D. A., Christensen-Dalsgaard, J., Ciardi, D., Dunham, E. W., Fressin, F., Gautier, III, T. N., Gilliland, R. L., Haas, M. R., Howell, S. B., Jenkins, J. M., Kjeldsen, H., Koch, D. G., Latham, D. W., Lissauer, J. J., Marcy, G. W., Rowe, J. F., Sasselov, D. D., Seager, S., Steffen, J. H., Torres, G., Basri, G. S., Brown, T. M., Charbonneau, D., Christiansen, J., Clarke, B., Cochran, W. D., Dupree, A., Fabrycky, D. C., Fischer, D., Ford, E. B., Fortney, J., Girouard, F. R., Holman, M. J., Johnson, J., Isaacson, H., Klaus, T. C., Machalek, P., Moorehead, A. V., Morehead, R. C., Ragozzine, D., Tenenbaum, P.,

- Twicken, J., Quinn, S., VanCleve, J., Walkowicz, L. M., Welsh, W. F., Devore, E., and Gould, A.: 2011, *ApJ* **729**, 27
- Batalha, N. M., Rowe, J. F., Bryson, S. T., Barclay, T., Burke, C. J., Caldwell, D. A., Christiansen, J. L., Mullally, F., Thompson, S. E., Brown, T. M., Dupree, A. K., Fabrycky, D. C., Ford, E. B., Fortney, J. J., Gilliland, R. L., Isaacson, H., Latham, D. W., Marcy, G. W., Quinn, S., Ragozzine, D., Shporer, A., Borucki, W. J., Ciardi, D. R., Gautier, III, T. N., Haas, M. R., Jenkins, J. M., Koch, D. G., Lissauer, J. J., Rapin, W., Basri, G. S., Boss, A. P., Buchhave, L. A., Charbonneau, D., Christensen-Dalsgaard, J., Clarke, B. D., Cochran, W. D., Demory, B.-O., Devore, E., Esquerdo, G. A., Everett, M., Fressin, F., Geary, J. C., Girouard, F. R., Gould, A., Hall, J. R., Holman, M. J., Howard, A. W., Howell, S. B., Ibrahim, K. A., Kinemuchi, K., Kjeldsen, H., Klaus, T. C., Li, J., Lucas, P. W., Morris, R. L., Prsa, A., Quintana, E., Sanderfer, D. T., Sasselov, D., Seader, S. E., Smith, J. C., Steffen, J. H., Still, M., Stumpe, M. C., Tarter, J. C., Tenenbaum, P., Torres, G., Twicken, J. D., Uddin, K., Van Cleve, J., Walkowicz, L., and Welsh, W. F.: 2012, *ArXiv e-prints*
- Beichman, C. A., Bryden, G., Gautier, T. N., Stapelfeldt, K. R., Werner, M. W., Misselt, K., Rieke, G., Stansberry, J., and Trilling, D.: 2005, *ApJ* **626**, 1061
- Beichman, C. A., Bryden, G., Stapelfeldt, K. R., Gautier, T. N., Grogan, K., Shao, M., Velusamy, T., Lawler, S. M., Blaylock, M., Rieke, G. H., Lunine, J. I., Fischer, D. A., Marcy, G. W., Greaves, J. S., Wyatt, M. C., Holland, W. S., and Dent, W. R. F.: 2006a, *ApJ* **652**, 1674
- Beichman, C. A., Tanner, A., Bryden, G., Stapelfeldt, K. R., Werner, M. W., Rieke, G. H., Trilling, D. E., Lawler, S., and Gautier, T. N.: 2006b, *ApJ* **639**, 1166
- Booth, M., Wyatt, M. C., Morbidelli, A., Moro-Martín, A., and Levison, H. F.: 2009, *MNRAS* **399**, 385
- Borucki, W. J., Koch, D., Basri, G., Batalha, N., Brown, T., Caldwell, D., Caldwell, J., Christensen-Dalsgaard, J., Cochran, W. D., DeVore, E., Dunham, E. W., Dupree, A. K., Gautier, T. N., Geary, J. C., Gilliland, R., Gould, A., Howell, S. B., Jenkins, J. M., Kondo, Y., Latham, D. W., Marcy, G. W., Meibom, S., Kjeldsen, H., Lissauer, J. J., Monet, D. G., Morrison, D., Sasselov, D., Tarter, J., Boss, A., Brownlee, D., Owen, T., Buzasi, D., Charbonneau, D., Doyle, L., Fortney, J., Ford, E. B., Holman, M. J., Seager, S., Steffen, J. H., Welsh, W. F., Rowe, J., Anderson, H., Buchhave, L., Ciardi, D., Walkowicz, L., Sherry, W., Horch, E., Isaacson, H., Everett, M. E., Fischer, D., Torres, G., Johnson, J. A., Endl, M., MacQueen, P., Bryson, S. T.,

- Dotson, J., Haas, M., Kolodziejczak, J., Van Cleve, J., Chandrasekaran, H., Twicken, J. D., Quintana, E. V., Clarke, B. D., Allen, C., Li, J., Wu, H., Tenenbaum, P., Verner, E., Bruhweiler, F., Barnes, J., and Prsa, A.: 2010, *Science* **327**, 977
- Borucki, W. J., Koch, D. G., Basri, G., Batalha, N., Boss, A., Brown, T. M., Caldwell, D., Christensen-Dalsgaard, J., Cochran, W. D., DeVore, E., Dunham, E. W., Dupree, A. K., Gautier, III, T. N., Geary, J. C., Gilliland, R., Gould, A., Howell, S. B., Jenkins, J. M., Kjeldsen, H., Latham, D. W., Lissauer, J. J., Marcy, G. W., Monet, D. G., Sasselov, D., Tarter, J., Charbonneau, D., Doyle, L., Ford, E. B., Fortney, J., Holman, M. J., Seager, S., Steffen, J. H., Welsh, W. F., Allen, C., Bryson, S. T., Buchhave, L., Chandrasekaran, H., Christiansen, J. L., Ciardi, D., Clarke, B. D., Dotson, J. L., Endl, M., Fischer, D., Fressin, F., Haas, M., Horch, E., Howard, A., Isaacson, H., Kolodziejczak, J., Li, J., MacQueen, P., Meibom, S., Prsa, A., Quintana, E. V., Rowe, J., Sherry, W., Tenenbaum, P., Torres, G., Twicken, J. D., Van Cleve, J., Walkowicz, L., and Wu, H.: 2011, *ApJ* **728**, 117
- Brown, T. M., Latham, D. W., Everett, M. E., and Esquerdo, G. A.: 2011, *AJ* **142**, 112
- Bryden, G., Beichman, C. A., Carpenter, J. M., Rieke, G. H., Stapelfeldt, K. R., Werner, M. W., Tanner, A. M., Lawler, S. M., Wyatt, M. C., Trilling, D. E., Su, K. Y. L., Blaylock, M., and Stansberry, J. A.: 2009, *ApJ* **705**, 1226
- Bryden, G., Beichman, C. A., Trilling, D. E., Rieke, G. H., Holmes, E. K., Lawler, S. M., Stapelfeldt, K. R., Werner, M. W., Gautier, T. N., Blaylock, M., Gordon, K. D., Stansberry, J. A., and Su, K. Y. L.: 2006, *ApJ* **636**, 1098
- Burns, J. A., Lamy, P. L., and Soter, S.: 1979, *Icarus* **40**, 1
- Burns, J. A., Showalter, M. R., Hamilton, D. P., Nicholson, P. D., de Pater, I., Ockert-Bell, M. E., and Thomas, P. C.: 1999, *Science* **284**, 1146
- Castelli, F. and Kurucz, R. L.: 2004, *ArXiv Astrophysics e-prints*
- Chu, Y.-H., Su, K. Y. L., Bilikova, J., Gruendl, R. A., De Marco, O., Guerrero, M. A., Updike, A. C., Volk, K., and Rauch, T.: 2011, *AJ* **142**, 75
- Defrère, D., Absil, O., Augereau, J. C., di Folco, E., Coudé Du Foresto, V., Le Bouquin, J. B., Mérand, A., and Mollier, B.: 2011, in *EPSC-DPS Joint Meeting 2011*, p. 1084
- Dent, W. R. F., Walker, H. J., Holland, W. S., and Greaves, J. S.: 2000, *MNRAS* **314**, 702
- Dodson-Robinson, S. E., Beichman, C. A., Carpenter, J. M., and Bryden, G.: 2011, *AJ* **141**,

- Fortney, J. J., Demory, B.-O., Désert, J.-M., Rowe, J., Marcy, G. W., Isaacson, H., Buchhave, L. A., Ciardi, D., Gautier, T. N., Batalha, N. M., Caldwell, D. A., Bryson, S. T., Nutzman, P., Jenkins, J. M., Howard, A., Charbonneau, D., Knutson, H. A., Howell, S. B., Everett, M., Fressin, F., Deming, D., Borucki, W. J., Brown, T. M., Ford, E. B., Gilliland, R. L., Latham, D. W., Miller, N., Seager, S., Fischer, D. A., Koch, D., Lissauer, J. J., Haas, M. R., Still, M., Lucas, P., Gillon, M., Christiansen, J. L., and Geary, J. C.: 2011, *ApJS* **197**, 9
- Hahn, J. M., Zook, H. A., Cooper, B., and Sunkara, B.: 2002, *Icarus* **158**, 360
- Hillenbrand, L. A., Carpenter, J. M., Kim, J. S., Meyer, M. R., Backman, D. E., Moromartín, A., Hollenbach, D. J., Hines, D. C., Pascucci, I., and Bouwman, J.: 2008, *ApJ* **677**, 630
- Holman, M. J., Fabrycky, D. C., Ragozzine, D., Ford, E. B., Steffen, J. H., Welsh, W. F., Lissauer, J. J., Latham, D. W., Marcy, G. W., Walkowicz, L. M., Batalha, N. M., Jenkins, J. M., Rowe, J. F., Cochran, W. D., Fressin, F., Torres, G., Buchhave, L. A., Sasselov, D. D., Borucki, W. J., Koch, D. G., Basri, G., Brown, T. M., Caldwell, D. A., Charbonneau, D., Dunham, E. W., Gautier, T. N., Geary, J. C., Gilliland, R. L., Haas, M. R., Howell, S. B., Ciardi, D. R., Endl, M., Fischer, D., Fürész, G., Hartman, J. D., Isaacson, H., Johnson, J. A., MacQueen, P. J., Moorhead, A. V., Morehead, R. C., and Orosz, J. A.: 2010, *Science* **330**, 51
- Krist, J. E., Stapelfeldt, K. R., Bryden, G., Rieke, G. H., Su, K. Y. L., Chen, C. C., Beichman, C. A., Hines, D. C., Rebull, L. M., Tanner, A., Trilling, D. E., Clampin, M., and Gáspár, A.: 2010, *AJ* **140**, 1051
- Krivov, A. V., Reidemeister, M., Fiedler, S., Löhne, T., and Neuhäuser, R.: 2011, *MNRAS* **418**, L15
- Lawler, S. M., Beichman, C. A., Bryden, G., Ciardi, D. R., Tanner, A. M., Su, K. Y. L., Stapelfeldt, K. R., Lisse, C. M., and Harker, D. E.: 2009, *ApJ* **705**, 89
- Lissauer, J. J., Fabrycky, D. C., Ford, E. B., Borucki, W. J., Fressin, F., Marcy, G. W., Orosz, J. A., Rowe, J. F., Torres, G., Welsh, W. F., Batalha, N. M., Bryson, S. T., Buchhave, L. A., Caldwell, D. A., Carter, J. A., Charbonneau, D., Christiansen, J. L., Cochran, W. D., Desert, J.-M., Dunham, E. W., Fanelli, M. N., Fortney, J. J., Gautier, III, T. N., Geary, J. C., Gilliland, R. L., Haas, M. R., Hall, J. R., Holman, M. J., Koch, D. G., Latham, D. W., Lopez, E., McCauliff, S., Miller, N., Morehead, R. C., Quintana, E. V., Ragozzine, D., Sasselov, D., Short, D. R., and Steffen, J. H.: 2011a, *Nature* **470**, 53

- Lissauer, J. J., Ragozzine, D., Fabrycky, D. C., Steffen, J. H., Ford, E. B., Jenkins, J. M., Shporer, A., Holman, M. J., Rowe, J. F., Quintana, E. V., Batalha, N. M., Borucki, W. J., Bryson, S. T., Caldwell, D. A., Carter, J. A., Ciardi, D., Dunham, E. W., Fortney, J. J., Gautier, III, T. N., Howell, S. B., Koch, D. G., Latham, D. W., Marcy, G. W., Morehead, R. C., and Sasselov, D.: 2011b, *ApJS* **197**, 8
- Lisse, C. M., Kraemer, K. E., Nuth, J. A., Li, A., and Joswiak, D.: 2007, *Icarus* **191**, 223
- Lisse, C. M., Wyatt, M. C., Chen, C. H., Morlok, A., Watson, D. M., Manoj, P., Sheehan, P., Currie, T. M., Thebault, P., and Sitko, M. L.: 2012, *ApJ* **747**, 93
- Lovis, C., Mayor, M., Pepe, F., Alibert, Y., Benz, W., Bouchy, F., Correia, A. C. M., Laskar, J., Mordasini, C., Queloz, D., Santos, N. C., Udry, S., Bertaux, J.-L., and Sivan, J.-P.: 2006, *Nature* **441**, 305
- Moldovan, R., Matthews, J. M., Gladman, B., Bottke, W. F., and Vokrouhlický, D.: 2010, *ApJ* **716**, 315
- Moór, A., Ábrahám, P., Derekas, A., Kiss, C., Kiss, L. L., Apai, D., Grady, C., and Henning, T.: 2006, *ApJ* **644**, 525
- Morton, T. D. and Johnson, J. A.: 2011, *ApJ* **738**, 170
- Ragozzine, D. and Holman, M. J.: 2010, *ArXiv e-prints*
- Raymond, S. N., Armitage, P. J., Moro-Martin, A., Booth, M., Wyatt, M. C., Armstrong, J. C., Mandell, A. M., Selsis, F., and West, A. A.: 2012, *ArXiv e-prints*
- Rhee, J. H., Song, I., and Zuckerman, B.: 2008, *ApJ* **675**, 777
- Rieke, G. H. and Lebofsky, M. J.: 1985, *ApJ* **288**, 618
- Sinclair, J. A., Helling, C., and Greaves, J. S.: 2010, *MNRAS* **409**, L49
- Skrutskie, M. F., Cutri, R. M., Stiening, R., Weinberg, M. D., Schneider, S., Carpenter, J. M., Beichman, C., Capps, R., Chester, T., Elias, J., Huchra, J., Liebert, J., Lonsdale, C., Monet, D. G., Price, S., Seitzer, P., Jarrett, T., Kirkpatrick, J. D., Gizis, J. E., Howard, E., Evans, T., Fowler, J., Fullmer, L., Hurt, R., Light, R., Kopan, E. L., Marsh, K. A., McCallon, H. L., Tam, R., Van Dyk, S., and Wheelock, S.: 2006, *AJ* **131**, 1163

- Wright, E. L., Eisenhardt, P. R. M., Mainzer, A. K., Ressler, M. E., Cutri, R. M., Jarrett, T., Kirkpatrick, J. D., Padgett, D., McMillan, R. S., Skrutskie, M., Stanford, S. A., Cohen, M., Walker, R. G., Mather, J. C., Leisawitz, D., Gautier, III, T. N., McLean, I., Benford, D., Lonsdale, C. J., Blain, A., Mendez, B., Irace, W. R., Duval, V., Liu, F., Royer, D., Heinrichsen, I., Howard, J., Shannon, M., Kendall, M., Walsh, A. L., Larsen, M., Cardon, J. G., Schick, S., Schwalm, M., Abid, M., Fabinsky, B., Naes, L., and Tsai, C.-W.: 2010, *AJ* **140**, 1868
- Wright, J. T., Fakhouri, O., Marcy, G. W., Han, E., Feng, Y., Johnson, J. A., Howard, A. W., Fischer, D. A., Valenti, J. A., Anderson, J., and Piskunov, N.: 2011, *PASP* **123**, 412
- Wyatt, M. C.: 2005, *A&A* **433**, 1007
- Wyatt, M. C.: 2008, *ARA&A* **46**, 339
- Wyatt, M. C., Smith, R., Greaves, J. S., Beichman, C. A., Bryden, G., and Lisse, C. M.: 2007, *ApJ* **658**, 569

Note added in proof: During the publication process the WISE full data release became available, which updates fluxes and upper limits for some of the systems analyzed here, and presents measurements for additional Kepler targets. In particular, the W3 and W4 measurements in the KOI 1099 system have become upper limits. Reanalysis of the revised and expanded dataset is presented in a forthcoming paper.

Table 3. WISE Data for Debris Disk Candidates

KOI	W1 flux [mJy]	W2 flux [mJy]	W3 flux [mJy]	W4 flux [mJy]
469	1.49 ± 0.05	0.83 ± 0.03	0.49 ± 0.07	< 1.2
559	2.31 ± 0.07	1.28 ± 0.04	0.60 ± 0.08	< 2.5
871	1.14 ± 0.04	0.63 ± 0.02	0.39 ± 0.08	< 2.5
904	1.94 ± 0.06	1.03 ± 0.04	0.22 ± 0.07^a	< 1.6
943	0.97 ± 0.03	0.51 ± 0.02	0.36 ± 0.07	1.5 ± 0.5^a
1020	8.85 ± 0.27	4.78 ± 0.15	0.95 ± 0.10	2.0 ± 0.5
1099	1.05 ± 0.04	0.69 ± 0.03	0.69 ± 0.09	1.4 ± 0.5^a
1564	1.11 ± 0.04	0.59 ± 0.02	0.29 ± 0.07	2.0 ± 0.6

Note. — Fluxes and flux uncertainties are approximate, estimated from the given WISE magnitudes and magnitude errors.

^aSNR<3